



# Rhodamine B aggregation in self-assembled multilayers induced by polyelectrolyte and interfacial fluorescence recognition for DNA

Sun Xiangying\*, Liu Bin, Zhang Ying

College of Material Science and Engineering, Huaqiao University, Xiamen 361021, China

## ARTICLE INFO

### Article history:

Received 13 January 2011

Received in revised form 14 May 2011

Accepted 19 May 2011

Available online 26 May 2011

### Keywords:

Rhodamine B

Self-assembled multilayers

Poly(4-styrenesulfonate)

DNA

Interfacial fluorescence recognition

## ABSTRACT

Photophysical properties of Rhodamine B bound to water-soluble polyanion sodium poly(4-styrenesulfonate) (PSS) in solution and Quartz/APES/PSS/RB SAMs were investigated. Experiments showed that Rhodamine B aggregated in Quartz/APES/PSS/RB SAMs and its fluorescence behavior was different from that in Quartz/APES/RB SAMs without PSS. The constructed Quartz/APES/PSS/RB SAMs were applied for label-free interfacial fluorescence sensing of DNA with extremely high sensitivity.

© 2011 Elsevier B.V. All rights reserved.

## 1. Introduction

Detection of specific oligonucleotide sequences has important applications in medical research and diagnosis, food and drug industry monitoring, and environmental monitoring [1–4]. Most assays identify specific sequence through hybridization of an immobilized probe to the target analyte after the latter has been modified with a covalently linked label such as a fluorescent tag [5,6]. However, the need of functionalizing dye-modified oligonucleotide probes added to the complexity, cost, and overall assay speed limited the effectiveness to such detection strategies. It is still desirable to develop sensitive, facile, and label-free strategies to nucleic acid assay [7–9]. Recently SAMs have received much attention in analytical chemistry [10,11] and fluorescent SAMs have actually been applied for highly sensitive chemo- and bio-sensing [12–14]. Herein, based on Rhodamine B (RB) as a fluorescent probe, we constructed RB SAMs for label-free fluorescent sensing of DNA.

Rhodamine B is an important fluorescent dye employed as a DNA marker or probe. As an aromatic molecule, its existing form depends on the concentration [15–19]. At low concentration of  $\leq 0.0001$  mol/L, RB exists in its monomeric form and is highly fluorescent with an emission band centered at 580 nm. At high concentration of  $\geq 0.005$  mol/L, however, aggregation occurs because of  $\pi$ – $\pi$  interactions the fluorescence intensity at high dye concentration decreases and the emission band shifts to the

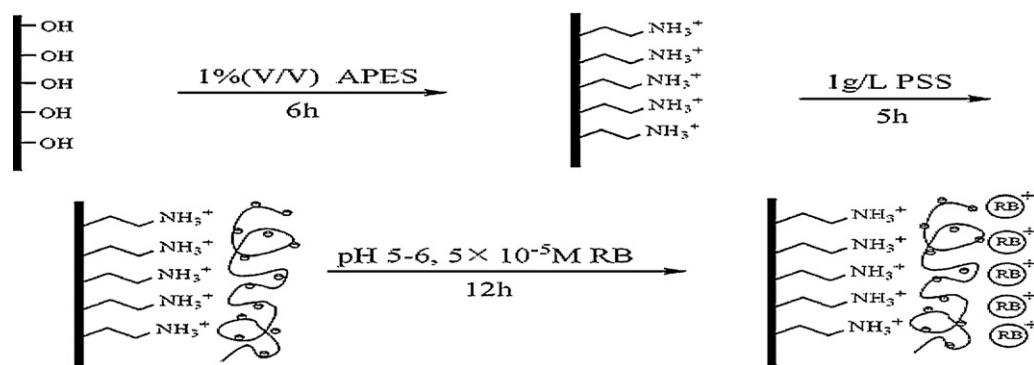
red with increasing dye concentration. Dye aggregation depends not only on dye concentration, but also on the medium [20–24]. Our experiments showed that the aggregation of RB dye in dilute solution takes place in the presence of a polyelectrolyte. Sodium poly(4-styrenesulfonate) (PSS), as a polyanion, was found to induce aggregation of RB at low concentration not only in solution, but also in SAMs. In this paper we focus our attention on the fluorescence behavior of RB in solution and in SAMs in the presence of the water-soluble polyanions PSS. Rhodamine B aggregated in Quartz/APES/PSS/RB SAMs, with a fluorescence emission different from that of Quartz/APES/RB SAMs without PSS. The constructed Quartz/APES/PSS/RB SAMs could be sensing for single- and double-stranded oligonucleotides (ssDNA and dsDNA) at the solid–liquid interface with extremely high sensitivity. Furthermore, it was found that the SAMs could be able to recognize specific DNA sequences by fluorescence response.

## 2. Experimental

### 2.1. Apparatus and reagents

Corrected fluorescence spectra were recorded on a Cary Eclipse fluorescence spectrophotometer (Varian, USA) with excitation wavelength of 530 nm and the slits of both 5 nm for excitation and emission. The angle between quartz plane and incident excitation light was set at  $50^\circ$  to ensure maximum efficiency of collecting emission light while avoiding reflection light interference. Fluorescence microscope images were obtained on Olympus B  $\times$  51 microscope (Olympus, Japan). Ultraviolet–visible absorption spec-

\* Corresponding author. Tel.: +86 595 22693548; fax: +86 592 6160088.  
E-mail addresses: [sunxy@hqu.edu.cn](mailto:sunxy@hqu.edu.cn), [liumy@hqu.edu.cn](mailto:liumy@hqu.edu.cn) (S. Xiangying).



**Scheme 1.** Procedures for RB-modified self-assembled multilayer film.

tra were recorded on UV-2550PC spectrophotometer (Shimadzu, Japan). Aqueous solutions were prepared using water obtained from a Millipore Milli-Q system (18 MΩ cm).

Fish sperm DNA (fsDNA) was purchased from Fluka Chemika Switzerland. ssDNA was prepared from fsDNA after boiling for 30 min and being frozen for 10 min to prevent DNA renaturation. DNA oligonucleotides were synthesized and purified by Sbsbio Technologies Inc. (Beijing, China). The sequences of the employed oligomers are given in Table 1.

Au nanoparticles (AuNP) were synthesized by means of citrate reduction of HAuCl<sub>4</sub> [25]. RB was purchased from China Guoyao Group, sodium poly(4-styrenesulfonate) (PSS, MW 70,000) was obtained from Acros, and γ-aminopropyltriethoxysilane (APES) was obtained from Shanghai Chemicals Co. Ltd. The other chemicals were of analytical grade or above.

## 2.2. Silanization of quartz wafers

Quartz wafers of 1 cm × 1 cm size were extensively washed with distilled water, ethanol each for 10 min. Cleaned wafers were then immersed in piranha solution 98% H<sub>2</sub>SO<sub>4</sub>/30% H<sub>2</sub>O<sub>2</sub> (7/3, V/V) for 10 min to protonate the quartz surface. Thus treated wafers were later cleaned by sonification in ultrapure water, dried with N<sub>2</sub>. Thus treated quartz wafers were immersed in 4% (v/v) aqueous solution of APES for 6 h to functionalize quartz surface with amino groups, which were finally washed by ultrapure water and dried with N<sub>2</sub>.

## 2.3. Preparation of Quartz/APES/RB SAMs

The silanized quartz wafer was dipped in 5.0 × 10<sup>−5</sup> mol/L RB solution of pH 10–11 for 2 h. The wafers were then taken out and left to dry in nitrogen, leading to Quartz/APES/RB SAMs.

## 2.4. Preparation of Quartz/APES/PSS/RB SAMs

The silanized quartz wafer was respectively dipped into PSS solution of 1 g/L for 5 h, 5.0 × 10<sup>−5</sup> mol/L RB solution of pH 5–6 for 12 h. The wafers were then taken out and left to dry in nitrogen, which leads to Quartz/APES/PSS/RB SAMs. The assembly process is depicted in Scheme 1.

**Table 1**  
Sequences of synthesized DNA.

Strands (12-mer)	Sequences
HS-DNA (probe)	5'-TAG GAA ACA CCA (CH <sub>2</sub> ) <sub>6</sub> -SH-3'
Complementary DNA (c-target)	TGG TGT TTC CTA
Noncomplementary DNA (nc-target)	AAA TAT CAT CTT

## 2.5. Preparation of Quartz/APES/PSS/RB/AuNP/Probe SAMs

The above prepared Quartz/APES/PSS/RB SAMs were immersed in synthesized AuNP solution for 3 h, 2.0 × 10<sup>−6</sup> mol/L HS-DNA probe was then dipped onto the surface of SAMs via Au-S chemical bonding. This allowed the construction of fluorescent multilayer film Quartz/APES/PSS/RB/AuNP/probe.

## 3. Results and discussion

### 3.1. Polyanion PSS induced RB aggregation in dilute solution

Usually the dye concentration exerts influence on its existing form, RB for example aggregating to dimer in concentrated solution. However, our experiments showed that polyelectrolyte PSS could induce RB to aggregate in dilute solution. Fig. 1 was the fluorescence spectra of 5 × 10<sup>−5</sup> mol/L RB solution containing PSS with different concentration, and showed that upon addition of PSS, fluorescence of RB was quenched and the emission wavelength shifted to the red, which suggested that, RB dimer was formed in dilute solution. Excess amount of PSS, however, induced the transformation of RB dimer into monomer, the fluorescence was hence recovered accompanied by a blue shift. The effect of PSS on RB was different from that on dyes, such as Acridine Orange, Thioflavin T [26]. PSS could induce Thioflavin T excimer formation, which may be ascribed to different dye structure and interaction between dye and PSS, could be explained by computational approach of quantum chemistry.

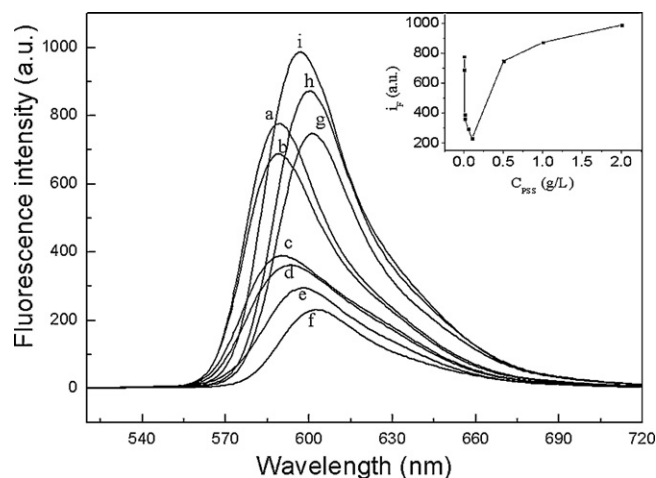


**Fig. 1.** Fluorescence spectra of RB in the presence of PSS of varying concentration. Inset shows the plot of RB fluorescence intensity versus PSS concentration. C<sub>PSS</sub> (g/L): (a) 0; (b) 0.001; (c) 0.005; (d) 0.01; (e) 0.05; (f) 0.1; (g) 0.5; (h) 1.0; (i) 2.0.

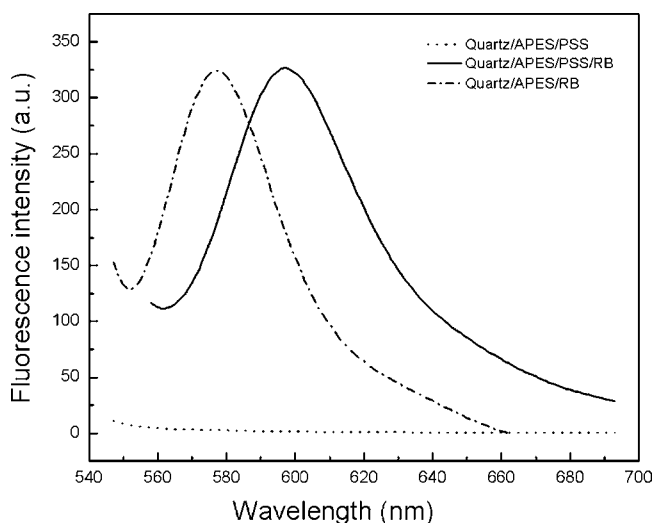


**Fig. 2.** Fluorescence spectra of Quartz/APES/PSS, Quartz/APES/RB and Quartz/APES/PSS/RB SAMs.

Similar change in the fluorescence spectra was also observed with Quartz/APES/PSS/RB SAMs, which means that PSS on the surface of silanized quartz wafer could induce RB aggregation in the film. In Quartz/APES/RB SAMs without PSS, however, RB at the same concentration exists in its monomer form.

### 3.2. Spectral properties of Quartz/APES/PSS/RB and Quartz/APES/RB SAMs

Surface fluorescence spectra of Quartz/APES/PSS, Quartz/APES/PSS/RB and Quartz/APES/RB films are shown in Fig. 2. It was found that Quartz/APES/PSS/RB and Quartz/APES/RB emitted RB-characteristic fluorescence, but Quartz/APES without RB was nonfluorescent, which proved that RB had been successfully assembled on the surface of quartz wafers in the cases of Quartz/APES/PSS/RB and Quartz/APES/RB SAMs. While fluorescence emission of Quartz/APES/RB peaked at 576 nm was observed, the maximum emission wavelength of Quartz/APES/PSS/RB was 596 nm. This indicates a substantial red shift in the presence of PSS, confirming that PSS indeed induced RB dimerization in Quartz/APES/PSS/RB SAMs. Fig. 3a and b were the fluorescence images of Quartz/APES/RB and Quartz/APES/PSS/RB SAMs, respectively, which supported this conclusion. In these images it was found that RB on the surface of Quartz/APES/PSS/RB well distributed with strong red fluorescence, the fluorescence color was the same as that of RB dimer solution whereas different from that of Quartz/APES/RB, which again confirmed the aggregation of RB in the Quartz/APES/PSS/RB SAMs. It shall be pointed out that, although pH of RB assembling solutions in two films (Quartz/APES/PSS/RB and Quartz/APES/RB) was not the same, experiments showed that the emission wavelength of RB was almost the same at pH higher than 3. The observed difference in the emission wavelengths of Quartz/APES/PSS/RB and Quartz/APES/RB thereby resulted from the action of PSS, and PSS in the Quartz/APES/PSS/RB SAMs induced RB aggregation.

The diffuse reflection–absorption spectra of Quartz/APES/PSS/RB and Quartz/APES/RB SAMs, showed in Fig. 4, also supported this conclusion.

Indeed, Fig. 4 shows that the absorption maximum of Quartz/APES/RB SAMs peaked at 558 nm is close to that of RB monomer in solution, while the absorption spectrum of Quartz/APES/PSS/RB SAMs is similar to that of RB dimer, clearly reflecting the role of PSS in inducing RB aggregation.

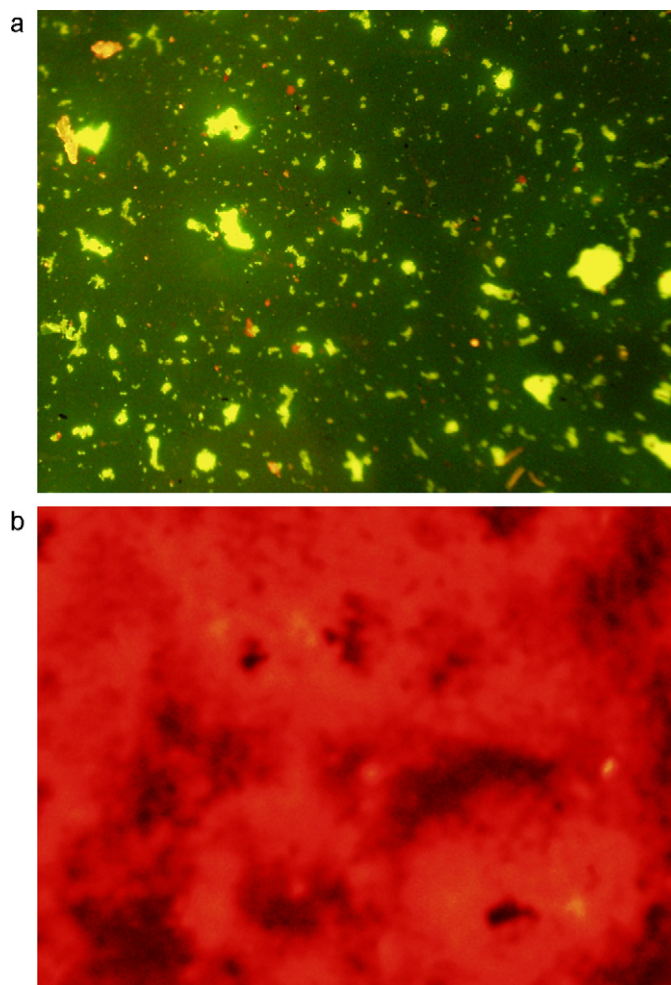


**Fig. 3.** Fluorescence images of (a) Quartz/APES/RB and (b) Quartz/APES/PSS/RB.

### 3.3. Fluorescence recognition for ssDNA and dsDNA based on Quartz/APES/PSS/RB SAMs

Since RB as a fluorescent probe for DNA, our past work had showed that the interfacial fluorescent sensing based on SAMs showed high sensitivity [12–14], thus a novel fluorescent recognition method was designed for ssDNA and dsDNA on the basis of

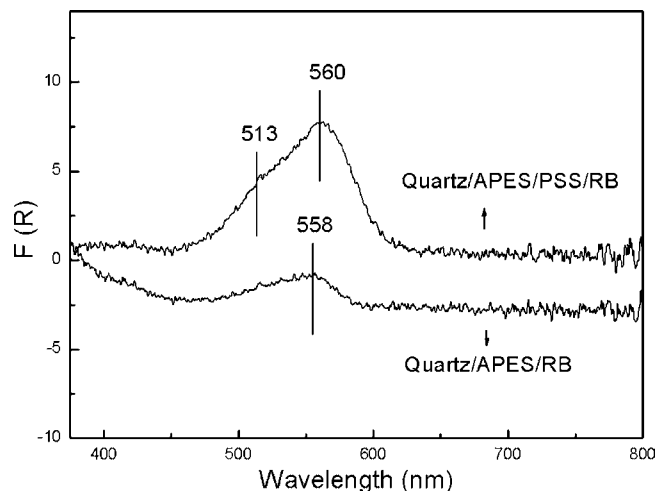


**Fig. 4.** Diffuse reflection–absorption spectra of SAMs.

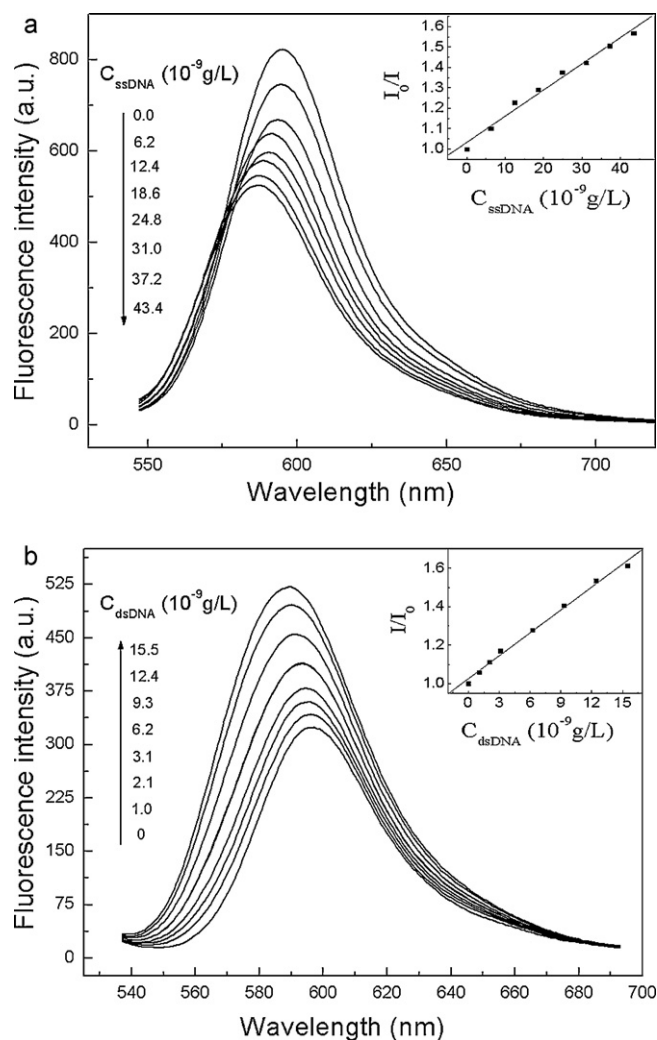


**Fig. 5.** Fluorescence spectra of Quartz/APES/PSS/RB in the presence of (a) ssDNA and (b) dsDNA at different concentration. Inset shows the linear correlation of fluorescence intensity with DNA concentration.

Quartz/APES/PSS/RB SAMs. Fig. 5 showed the fluorescence spectra of Quartz/APES/PSS/RB in 0.01 M Tris–HCl buffer solution of pH 7.4 containing DNA with different concentration. Comparing the fluorescence spectra of Fig. 5a and b, it was found that the fluorescence of Quartz/APES/PSS/RB SAMs was enhanced upon addition of dsDNA, whereas it was quenched in the presence of ssDNA, which was similar to that observed with the RB dimer in solution in its fluorescence response towards DNA, but opposite to that observed with Quartz/APES/RB [27]. This again reflects PSS induced aggregation of RB in Quartz/APES/PSS/RB film. The observed small blue-shift of the fluorescence emission after the addition of DNA might be ascribed to the dissociation of RB dimer. The completely different fluorescence response of Quartz/APES/PSS/RB with ssDNA and dsDNA may be due to the different binding interaction modes of RB with ssDNA and dsDNA and secondary structure discrepancy between ssDNA and dsDNA [27].

Generally speaking, there are three kinds of uncovalent binding modes of DNA and small molecules, electrostatic bonding, groove contact and intercalation action. It suggests probable that RB dimer molecular effectively interacted strongly with dsDNA in intercalation action predominant [28]. Increases in temperature will damage ordered-arrangement of base pairs and also serve to break secondary structure in dsDNA chains, and then the disappeared groove contact influence on binding modes of DNA

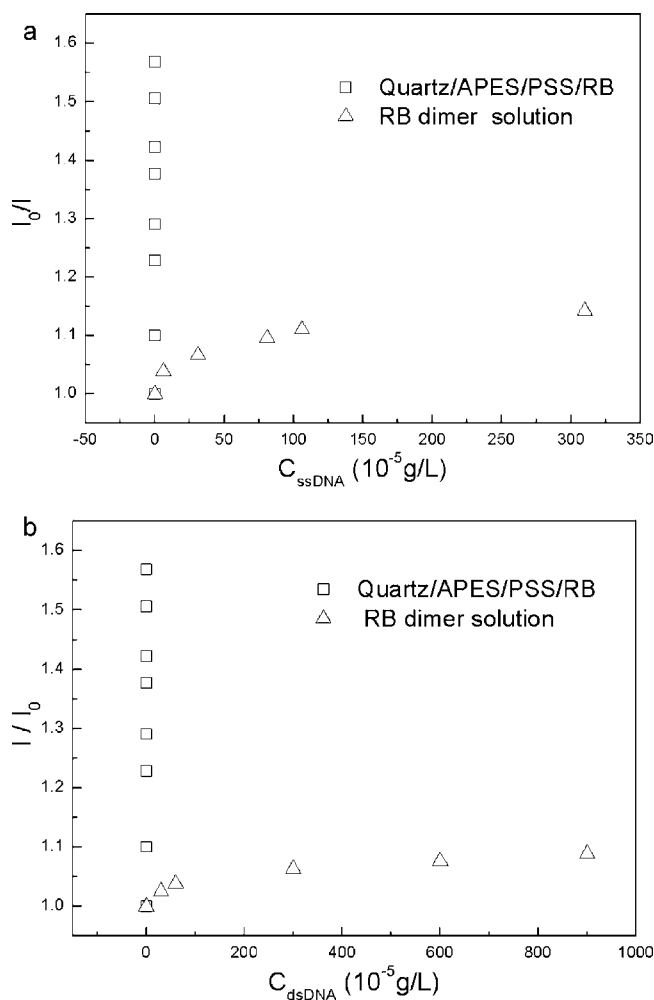


**Fig. 6.** Relationship of  $I_0/I$  of Quartz/APES/PSS/RB (□), RB dimer in solution of  $1.00 \times 10^{-3}$  mol/L (Δ) with the concentration of (a) ssDNA and (b) dsDNA.

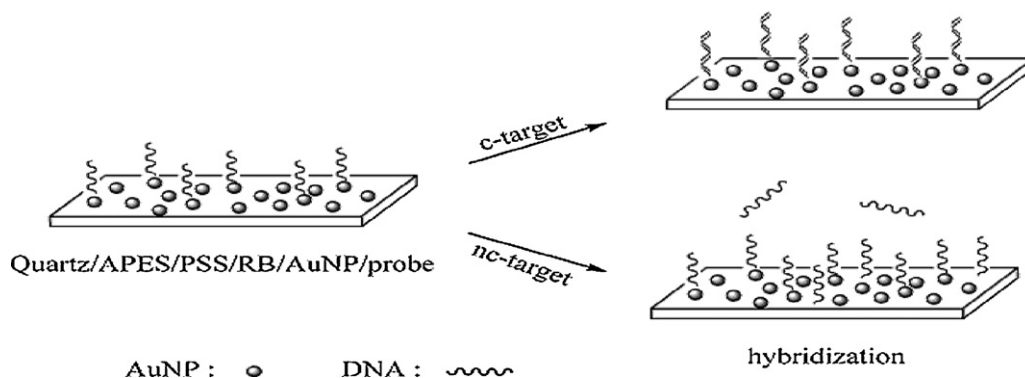
and Quartz/APES/PSS/RB. Under this situation, RB has interacted weakly with bases directly by hydrogen bond, ionic bond and hydrophobic bond, coordinated with the negatively charged phosphate backbone, which all most exposed to the aqueous solution. Then different fluorescence response efficiency from dsDNA was obtained.

Further experiments showed that the interfacial fluorescence recognition can indeed be established for ssDNA and dsDNA by monitoring the change in the fluorescence of Quartz/APES/PSS/RB SAMs. As shown in insert of Fig. 5, a good linear correlation exists between relatively fluorescence intensity and DNA concentration over  $6.20 \times 10^{-9}$  to  $4.34 \times 10^{-8}$  g/L for ssDNA with a detection limit (3SD/K) of  $3.95 \times 10^{-10}$  g/L, and over  $1.00 \times 10^{-9}$  to  $1.55 \times 10^{-8}$  g/L for dsDNA with a detection limit (3SD/K) of  $2.79 \times 10^{-10}$  g/L, respectively,  $I$  and  $I_0$  represents the fluorescence intensity in the presence and absence of DNA. Compared with solution-phase RB-based fluorescent sensing, the sensitivity of the Quartz/APES/PSS/RB SAMs based method is higher by 5 orders of magnitude than that of RB dimer in solution, as clearly seen in Fig. 6.

### 3.4. Label-free fluorescence recognition for DNA sequence

Based on the recognition capability of RB SAMs for DNA, we developed a label-free fluorescence method to detect oligonucleotide sequence. Quartz/APES/PSS/RB/AuNP/probe SAMs was constructed according to the experimental 2.3, and immersed





**Scheme 2.** Diagram of fluorescence recognition by Quartz/APES/PSS/RB/AuNP/probe for specific DNA sequences.

into 0.01 mol/L Tris-HCl buffer solution of pH 7.8 containing 0.3 mol/L NaCl. The target DNA in Table 1 was added into the solution and hybridized with the probe in SAMs. The optimal hybridization temperature was at about 20 °C, the hybridization time was 18 h. Fig. 7a and b were the fluorescence spectra of Quartz/APES/PSS/RB/AuNP/probe in the presence of c-target and nc-target with different concentration, respectively, and we found that the fluorescence intensity increased upon addition of the complementary target (c-target), whereas it decreased in the pres-

ence of the non-complementary target (nc-target). This might be explained that the HS-DNA probe in the SAMs hybridized with c-target to dsDNA, and the effect of c-target addition was similar to that of dsDNA on SAMs. A linear relationship between the relative fluorescence intensity  $I/I_0$  and c-target concentration over  $2.0 \times 10^{-12}$  to  $2.0 \times 10^{-11}$  mol/L was found (showed in the inset of Fig. 7a), with a limit of detection (3SD/K) of  $5.2 \times 10^{-13}$  mol/L, which demonstrates a hybridization method of SAMs based with higher analytical sensitivity. The probe in SAMs, however, did not hybridize with nc-target, the effect of nc-target addition was therefore similar to that of ssDNA on SAMs (Scheme 2).

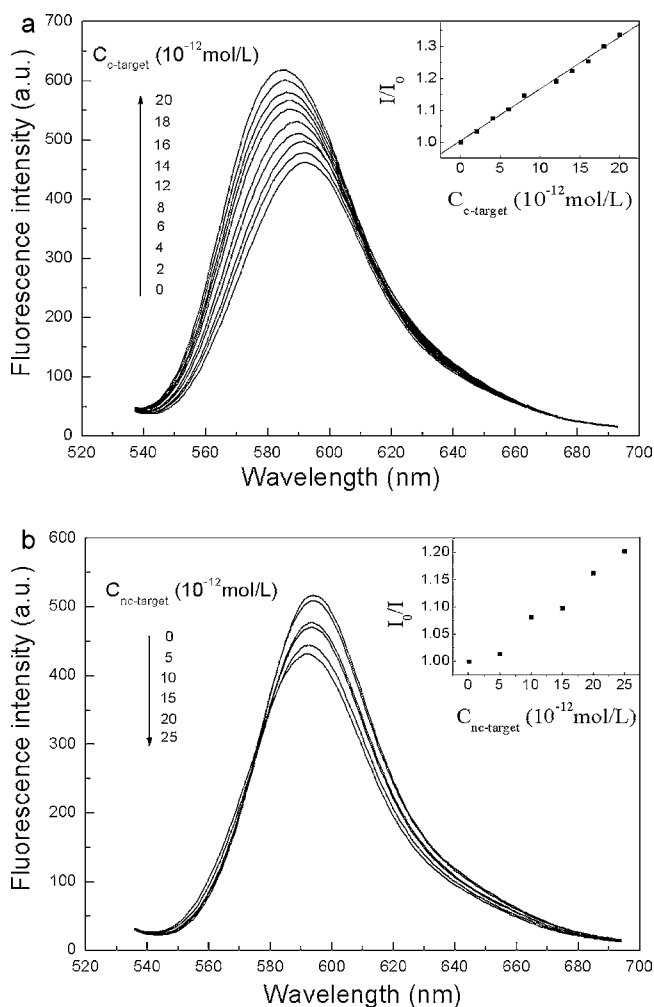


**Fig. 7.** Fluorescence spectra of Quartz/APES/PSS/RB/AuNP/probe in the presence of (a) c-target and (b) nc-target at different concentration. Inset shows the linear correlation of fluorescence intensity against target DNA concentration.

#### 4. Conclusions

In the presence of polyanionic PSS, RB aggregation was found not only in dilute solution but also in SAMs. The fluorescence spectra of RB SAMs from the same concentration RB assembling solution in the presence PSS is different from that in the absence of PSS. The constructed Quartz/APES/PSS/RB SAMs has the fluorescence behavior similar to that of RB dimer solution, and can recognize ssDNA and dsDNA at solid-liquid interface, but SAMs based show extremely high sensitivity. We have utilized these observations to design a simple, fast assay for DNA recognition with inexpensive commercially available materials, which eventually allows for a label free detection of DNA based on this SAMs interfacial sensing protocol. Furthermore, fluorescence recognition for specific DNA sequences on-line could also be done.

#### Acknowledgements

This work was supported by the National Natural Science Foundation of China (grant nos. 20955001 and 20575023), the Major Research Plan of National Nature Science Foundation of China (grant no. 90922028), Natural Science Foundation of Fujian Province (grant no. D0810016), Foundation of Overseas-Chinese Affairs Office of the State Council of China (grant no. 09QZR05), and Scientific Research Foundation for the Returned Overseas Chinese Scholars, Ministry of Education of China.

#### References

- [1] J.B. Lee, M.J. Campolongo, J.S. Kahn, Y.H. Roh, M.R. Hartman, D. Luo, *Nanoscale* 2 (2010) 188–197.
- [2] N.C. Seeman, *Nature* 421 (2003) 427–431.
- [3] M. Famulok, J.S. Hartig, G. Mayer, *Chem. Rev.* 107 (2007) 3715–3743.
- [4] R.A. Potyrailo, R.C. Conrad, A.D. Ellington, G.M. Hieftje, *Anal. Chem.* 70 (1998) 3419–3425.
- [5] S. Berndt, H.A. Wagenknecht, *Angew. Chem. Int. Ed.* 48 (2009) 2418–2421.
- [6] J.L. He, Z.S. Wu, S.B. Zhang, G.L. Shen, R.Q. Yu, *Talanta* 80 (2010) 1264–1268.
- [7] X. Xu, M.S. Han, C.A. Mirkin, *Angew. Chem., Int. Ed.* 46 (2007) 3468–3470.
- [8] F. Pu, D. Hu, J.S. Ren, S. Wang, X.G. Qu, *Langmuir* 26 (2010) 4540–4545.

- [9] N. Akbay, M.Y. Losytsky, V.B. Kovalska, A.O. Balanda, S.M. Yarmoluk, J. Fluoresc. 18 (2008) 139–147.
- [10] J.J. Gooding, F. Mearns, W.R. Yang, J.Q. Liu, Electroanalysis 15 (2003) 81–96.
- [11] S. Flink, F.C.J.M. van Veggel, D.N. Reinhoudt, Adv. Mater. 12 (2000) 1315–1328.
- [12] X.Y. Sun, K.H. Xia, B. Liu, Talanta 76 (2008) 747–751.
- [13] X.Y. Sun, B. Liu, Y.B. Jiang, Anal. Chim. Acta 515 (2004) 285–290.
- [14] X.Y. Sun, B. Liu, F. He, Thin Solid Films 516 (2008) 2213–2217.
- [15] I.L. Arbeloa, P.R. Ojeda, Chem. Phys. Lett. 87 (1982) 556–560.
- [16] F.L. Arbeloa, P.R. Ojeda, I.L. Arbeloa, J. Lumin. 44 (1989) 105–112.
- [17] N.O. Mchedlov-Petrosyan, N.A. Vodolazkaya, A.O. Doroshenko, J. Fluoresc. 13 (2003) 235–248.
- [18] N.O.M. Petrossyan, Y.V. Kholin, Russ. J. Appl. Chem. 77 (2004) 414–422.
- [19] P. Ilich, P.K. Mishra, S. Macura, T.P. Burghardt, Spectrochim. Acta, Part A 52 (1996) 1323–1330.
- [20] T.D. Slavnova, A.K. Chibisov, H. Görner, J. Phys. Chem. A 106 (2002) 10985–10990.
- [21] I. Moreno-Villoslada, M. Jofre, V. Miranda, R. Gonzalez, T. Sotelo, S. Hess, B.L. Rivas, J. Phys. Chem. B 110 (2006) 11809–11812.
- [22] M.G. Neumann, C.C. Schmitt, E.T. Iamazaki, J. Colloid Interface Sci. 264 (2003) 490–495.
- [23] K. Ikegami, Curr. Appl. Phys. 6 (2006) 813–819.
- [24] K. Ray, H. Nakahara, J. Phys. Chem. B 106 (2002) 92–100.
- [25] G. Frens, Nat. Phys. Sci. 241 (1973) 20–22.
- [26] D. Li, X.Y. Sun, F. Li, Spectrosc. Spect. Anal. 31 (2011) 431–435.
- [27] Y. Zhang, X.Y. Sun, B. Liu, Chin. J. Anal. Chem. 37 (2009) 665–670.
- [28] H. Sugiyama, C. Lian, M. Isomura, I. Saito, A.H.J. Wang, Proc. Natl. Acad. Sci. U.S.A. 93 (1996) 14405–14410.